Optik - International Journal for Light and Electron Optics 287 (2023) 171032

Contents lists available at ScienceDirect

Optik

journal homepage: www.elsevier.com/locate/ijleo

(Invited) control of supercontinuum generation due to soliton propagation in fibers with varying dispersion

D. Korobko [a], V. Kamynin [b], M. Salganski [c], A. Sysoliatin [b,*], I. Zhluktova [b], A. Zverev [b], I. Zolotovskii [a], V. Tsvetkov [b]

[a] Ulyanovsk State University, 432017 Ulyanovsk, Russia
[b] Prokhorov General Physics Institute, Russian Academy of Sciences, 119991 Moscow, Russia
[c] G.G. Devyatykh Institute of Chemistry of High-Purity Substances, Russian Academy of Sciences, 603950 Nizhny Novgorod, Russia

ARTICLE INFO

Keywords:
Optical soliton
Fiber laser
Dispersion varying fiber
Supercontinuum

ABSTRACT

We demonstrate experimental and numerical studies of supercontinuum generation for silica fibers with longitudinally varying diameter and dispersion. The significant difference in the spectral and temporal transformations of the pump pulse depending on the direction of propagation in the researched fiber samples is shown. Numerical simulations demonstrate the possibility of the supercontinuum spectra management by controlling the longitudinal profile of the fiber. Ways to optimize the output in terms of spectral flatness and efficient energy transfer to the desired wavelength region are presented.

1. Introduction

Typical features of nonlinear optical processes are spectrum broadening and generation of new spectral components. These effects are most pronounced in optical fibers, where the waveguide nature of light propagation pushes the power thresholds for nonlinear interactions towards their lower limits. Progress in fiber optic technology and the availability of fibers with a variety of performance characteristics make them ideal media for studies of broadband optical supercontinuum (SC) generation [1–3]. In recent decades, optical fiber SC generation has become the subject of research for many scientific groups, since this topic is of interest in various applications, for example, remote sensing [4], respiration analysis [5], spectroscopy and residual gas detection [6], hyperspectral microscopy [7], early diagnosis of diseases [8], coherence tomography [9], optical communications [10], etc.

Considering the problem of the SC generation in the telecom range ($\lambda \sim 1.53 - 1.56$ μm) we should note its particular importance for applications in wavelength division multiplexing systems strongly required high flatness of generated SC spectrum [11–13]. A number of works have shown that longitudinally non-uniform silica fibers are extremely attractive for such applications [14–18]. In this paper, we report on experimental and theoretical studies of laser pulses propagation in fibers with longitudinally varying profiles. It is known that this kind of optical fibers have already been reported for the generation of parabolic pulses (in normal decreasing dispersion fibers) [19,20], for reduction of intra-pulse optical chirp (in active normal dispersion increasing fibers) [21,22], and for compression of chirped similariton sech^2-shaped pulses (in anomalous decreasing dispersion fibers) [23–26]. The practical way to develop dispersion varying fibers with arbitrary longitudinal profiles of the dispersion (e.g., periodically oscillating dispersion) has been well established [27,28].

* Corresponding author.
E-mail address: alexs@fo.gpi.ru (A. Sysoliatin).

https://doi.org/10.1016/j.ijleo.2023.171032
Received 11 March 2023; Accepted 31 May 2023
Available online 1 June 2023

The typical mechanism for SC generation by subpicosecond laser pulses is higher-order soliton fission, which occurs during the propagation of *N*-soliton pulse in a fiber with anomalous dispersion. The delayed nonlinear response and the dependence of group velocity dispersion (GVD) on wavelength are the basic factors contributing to the soliton fission dynamics. The first factor causes Raman-induced shift of the soliton spectrum to longer wavelengths. The second is responsible for energy exchange between solitons and linear optical waves, which leads to generation of dispersive waves in the spectral range near the zero dispersion wavelength [1, 12,29,30]. In the paper, we consider examples of these processes occurring in a silica fiber with a longitudinally varying diameter. A principal feature of our work is the investigation of various experimental configurations associated with the original master-oscillators (MOs) of different spectral ranges. In the first case, we use the MO of standard telecom range, so the pump pulse propagates in anomalously dispersion decreasing (or increasing) fiber experiencing typical stages of *N*-soliton fission [1,12,14,31]. In the second case, a relatively high-energy pulse at the wavelength of 1060 nm enters initially into the region of normal dispersion region of the fiber. As a result, at the output we observed broadband SC generation in the range of 900 – 2400 nm [32]. A comparison of the forward and backward pump pulse propagation for the configurations considered provides important information about the efficient pump pulse conversion into the broad SC due to the *N*-soliton compression, soliton self-frequency Raman shift and dispersion wave generation.

2. Experiment

We built the experimental SC sources using the standard scheme consisting of an MO, a fiber amplifier, and a nonlinear medium (dispersion varying fiber). The use of silica-based fibers allows the realization of an all-fiber configuration without mechanical connections and bulk optics.

The used sample of dispersion varying fiber was produced in the GPI RAS and IHPS RAS by the taper-type technique of fiber drawing, that allowed a smooth linear change in core diameter from 6 to 9 μm to be maintained [28]. The fiber sample with a total length of 78 m has a longitudinal profile with a linearly increasing cladding diameter from 120 μm to 150 μm on the fiber ends. The estimation of the fiber dispersion can be made from the Fig. 2(c) that shows the dispersion curves for similar single-mode fibers of specified diameters. As one can see, the dispersion of the fiber at the wavelength of 1530 nm increases linearly from 0 (at the fiber end with diameter 120 μm) to 11 ps/nm/km (at 150 μm fiber end). We consider the pump pulse propagation from 150 μm to 120 μm fiber end as the forward direction in fiber with decreasing of anomalous dispersion (dispersion decreasing fiber - DDF) and propagation from 120 μm to 150 μm fiber end as backward direction corresponding to increasing of anomalous dispersion (dispersion increasing fiber - DIF).

The MO in the first configuration (Fig. 1(a)) generates pulses of 1.3 ps at a wavelength of 1529 nm with repetition rate of ~ 92 MHz. The power launched into dispersion varying fiber is controlled by the power of the pump laser diode (LD). The spectrum corresponding to the launched power ~ 10.5 mW is shown in Fig. 2(a). The − 3 dB pulse spectrum width is about 3.5 nm. The time bandwidth product of the ~0.585 shows that the output pulse is slightly chirped, which is also confirmed by FROG-trace (see inset of Fig. 2b).

We estimate that the pump pulse at the input of the variable dispersion fiber experiences an insertion loss of ~30 %. Fig. 3(a, b) show the spectra at the DDF and DIF outputs, respectively. During forward propagation of the pump pulse, at the DDF output one can observe wide SC spectra corresponding to an average output power of ~ 5 mW. In the case of backward propagation, the generated spectrum is much narrower, despite the higher output power (~ 6.4 mW). The spectrogram obtained for the forward propagation (Fig. 4(a)) shows that source of the broad SC is the ultrashort single pulse accompanied by patchy background. The spectrogram corresponding to the backward propagation shows generation of at least two pulses (Fig. 4(b)).

The second configuration based on Yb MO (Fig. 1(b)) with pulses repetition rate of ~1 MHz has the output spectrum centered at the wavelength of 1063 nm. The ytterbium-doped fiber amplifier allows increasing the average power up to 800 mW with pulse energy of ~0.8 μJ. Fig. 2(b) shows the oscilloscope trace (see inset) and the spectrum of the output pulse. As we believe, the strongly asymmetrical shape of the pulse spectrum caused by the action of stimulated Raman scattering (SRS), in particular, intense band centered at the wavelength of 1120 nm relates to the 1st Stokes component.

As in the previous case, insertion losses at the dispersion varying fiber input were rather significant (more than 30 %). The SC spectra obtained at the fiber output for different directions of pump pulse propagation are shown in Fig. 5(a, b). Structure of both

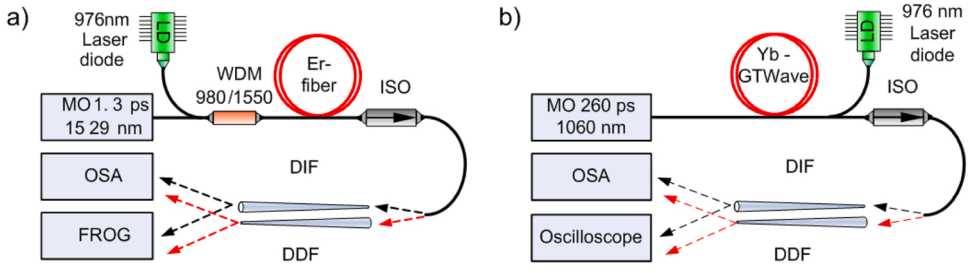

Fig. 1. Experimental setup. (a) SC generator of telecom range. (b) SC generator with master-oscillator at the wavelength of 1060 nm. LD - pump laser diodes, DIF – dispersion increasing fiber, DDF – dispersion decreasing fiber.

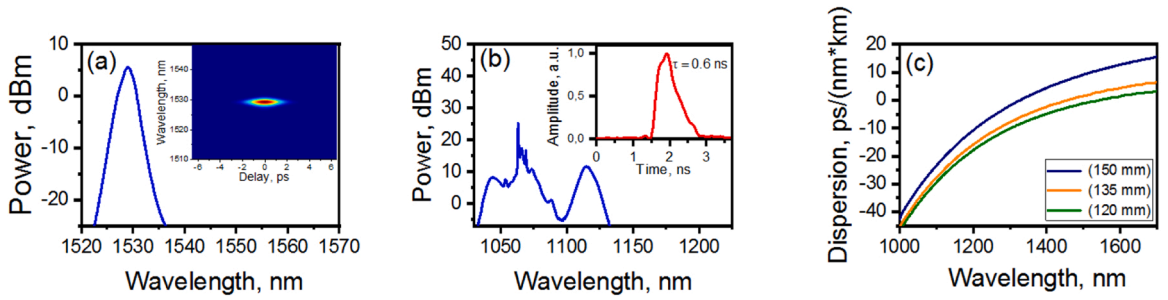

Fig. 2. (a) Spectrum and spectrogram of the pulse at the input of dispersion variable fiber for SC generator of telecom range. (b) Spectrum and envelope of the pulse at the input of dispersion varying fiber for SC generator with master-oscillator at the wavelength of 1060 nm. (c) Dispersion curves for single-mode fibers of the same structure as used dispersion varying fiber. Curves for the fibers with diameters 120 μm (green), 135 μm (orange) and 150 μm (blue) are shown.

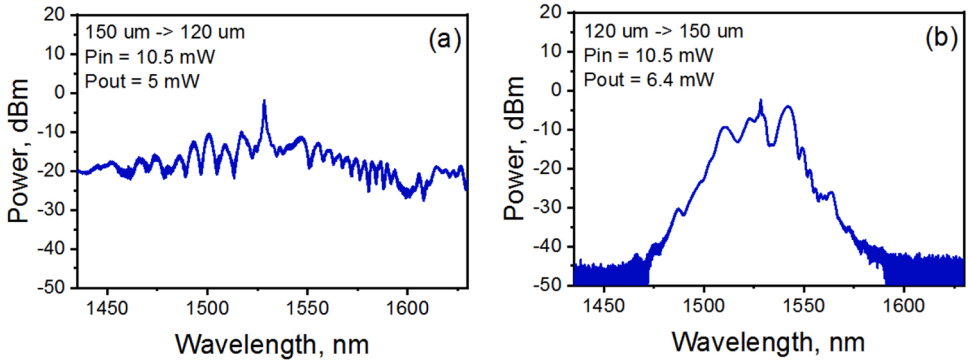

Fig. 3. SC optical spectra obtained for the propagation of the pump pulse with central wavelength of 1529 nm in DDF (a), in DIF (b).

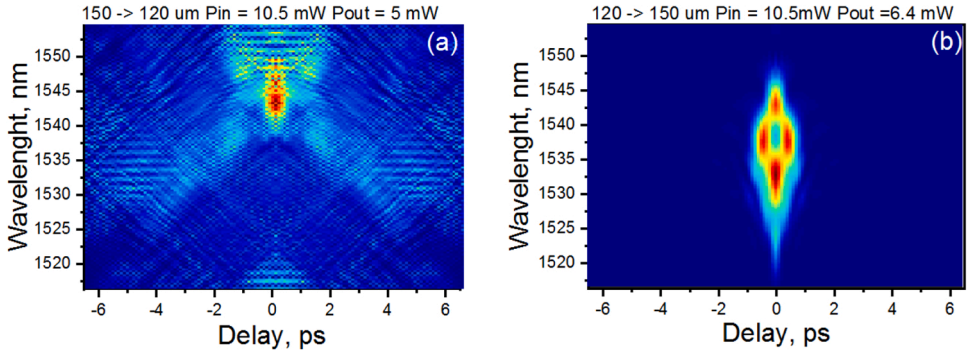

Fig. 4. Spectrograms obtained for the propagation of the pump pulse with central wavelength of 1529 nm in DDF (a), in DIF (b).

spectra is similar. Several intense bands in the range of 1063–1250 nm relate to sequential orders of SRS originated from the pump pulse spectrum. In the range of anomalous dispersion ($\lambda > 1500$nm), one can observe broad flat spectral plateau spreading into the area with wavelength $\lambda > 2000$ nm. It is important to note that for backward pump pulse propagation this spectral plateau has a significantly larger width with a long-wave boundary close to 2400 nm. On the contrary, pump pulse propagating in forward direction provides the generation of short-wavelength SC band near the 950 nm (Fig. 5(a)).

Oscilloscope traces presented in Fig. 5 demonstrate the pulse envelopes observed at the output of dispersion varying fiber. In case of forward propagation pulse duration does not exceed 740 ps (Fig. 5(c)), but for backward propagation it grows up to ~ 1 ns (Fig. 5(d)). This can be explained by the wider spectrum at the output of DIF, where the spectral components of the pump pulse are more strongly stretched in time.

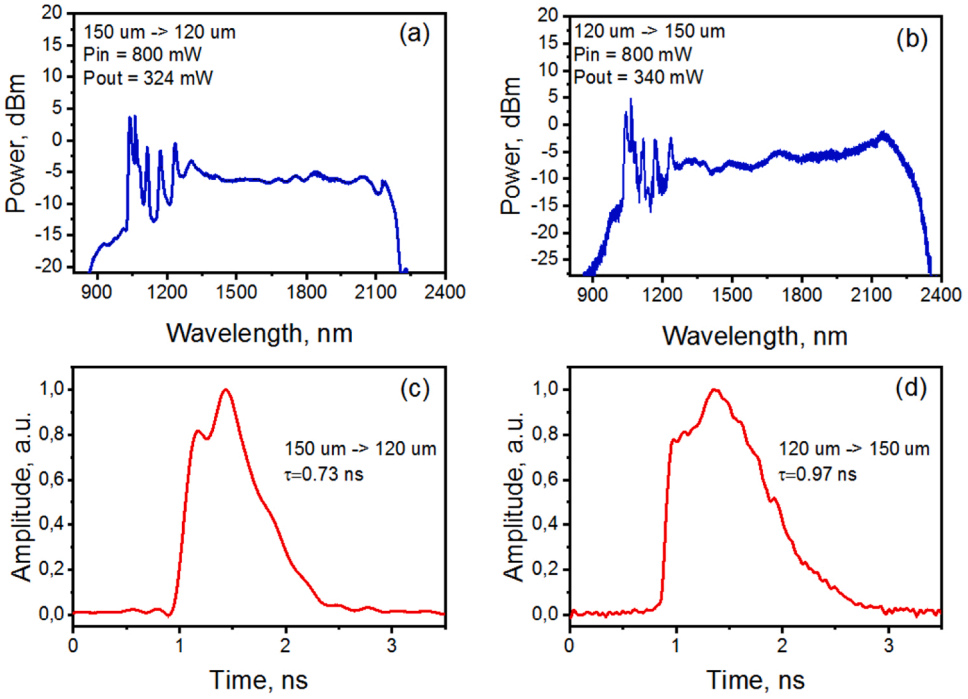

Fig. 5. The comparison of the SC spectra obtained at the output of dispersion varying fiber for forward (DDF) (a) and backward (DIF) (b) pump pulse propagation. Pulse envelopes obtained at the output of dispersion varying fiber for forward (c) and backward (d) pump pulse propagation. FWHM pulse durations are shown.

3. Numerical simulations

For a better understanding of the processes occurring during the SC generation, a numerical simulations of pump pulse propagation in an experimental sample of dispersion varying fiber. We performed it on the base of well-known generalized nonlinear Schrödinger

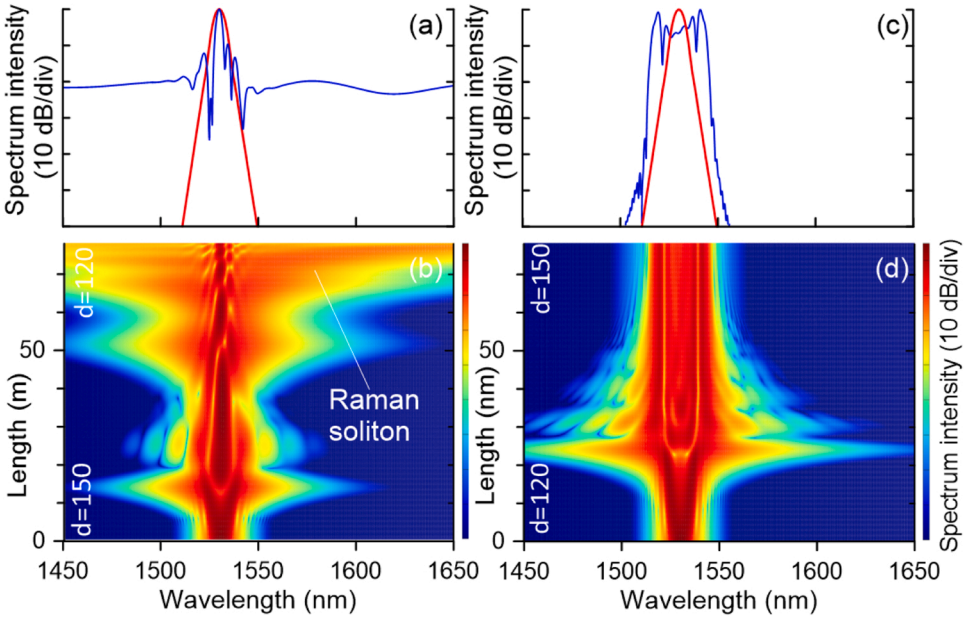

Fig. 6. Propagation of the pump pulse with central wavelength $\lambda = 1530$ nm in dispersion varying fiber. Results of numerical simulations. The pulse propagates in the DDF (a, b) or in the DIF (c, d). (a, c) Pulse spectrum at the input (red) and at the output of the fiber (blue line). (b, d) Evolution of the spectrum intensity during pump pulse propagation.

equation (NSE) for the field amplitude $A(z,t)$. This type of the NSE takes into account higher orders of dispersion, Raman scattering and nonlinearity dispersion [1,2,33,34]:

$$\frac{\partial A}{\partial z} - \sum_{k\geq 2} \frac{i^{k+1}\beta_k(z)}{k!}\frac{\partial^k A}{\partial t^k} - \frac{lA}{2} = i\gamma(z)\left(1+\frac{i}{\omega_0}\frac{\partial}{\partial t}\right)\left(A\int_{-\infty}^{\infty} R(t')|A(z,t-t')|^2 dt'\right) \quad (1)$$

Here, ω_0 is the carrier frequency,

$$R(t) = 0.82\cdot\delta(t) + 0.18\cdot\frac{\tau_1^2+\tau_2^2}{\tau_1\tau_2^2}\exp(-t/\tau_2)\sin(t/\tau_1)\Theta(t)$$

is the Raman response function, where the parameters $\tau_1 = 12.2$fs, $\tau_2 = 32$fs correspond to the silica fiber response, $\Theta(t)$ and $\delta(t)$are the Heaviside and Delta functions, respectively. The dispersive parameters$\beta_k(z)$ ($\beta_2$is the group velocity dispersion, β_3 is the third order dispersion, etc., $k \leq 8$) are determined by the longitudinal profile of cladding diameter$d(z)$. The β_k values for the diameters shown in Fig. 2(c) are obtained from polynomial approximation of dispersion curves and taken as the references. The intermediate values are calculated by second-order interpolation. The Kerr nonlinearity parameter γ also depends on the outer cladding diameter and here is assumed to be linearly growing in the forward fiber direction from the value $\gamma = 7\ \ \mathrm{W^{-1}km^{-1}}$ up to the value$\gamma = 9\ \ \mathrm{W^{-1}km^{-1}}$; l is the loss in the fiber (~1 dB/km).

For the first configuration with the pump at the wavelength of 1530 nm, the input pulse is specified in the form of chirped N-soliton pulse $A(t) = \sqrt{P_0}\,\mathrm{sech}(t/\tau)\exp(-iCt^2/2\tau^2)$ with duration $\tau = 0.75$ps, chirp $C = 1.5$ and peak power $P_0 = 30$W. Results of simulation of the pulse propagation are shown in Figs. 6 and 7. One can see several stages of the pulse evolution process. At the first stage, the initial pump pulse is compressed due to cooperation of the self-phase modulation and anomalous dispersion, and its spectrum is strongly broadened. In the next stage of soliton fission, the fundamental soliton is detached from the pump pulse. After soliton fission, the detached soliton propagates separately due to a Raman-induced frequency shift.

Significant differences in the propagating pulse evolution for forward and backward directions relate to the difference in longitudinal distribution of dispersion and nonlinearity. It is known that in uniform fiber the length of Raman soliton formation can be estimated as $L_R = \tau/\sqrt{\gamma P_0|\beta_2|}$ [35]. Significantly higher dispersion at the beginning of the DDF ensures that the soliton fission occurs much faster than in the DIF. Besides that, the detached Raman soliton experiences either adiabatic compression (in the DDF forward propagation) or broadening (for backward propagation) [25,36,37]. The case under consideration when one of fiber ends has zero dispersion is quite remarkable. The results of forward and backward propagation are drastically different. As one can see, the forward pump pulse evolution in the DDF provides the formation of a single ultrashort Raman soliton with a broad continuum spectrum. Whereas, backward propagation leads to the pulse decay with rather narrow spectrum width. The simulation results are quite similar

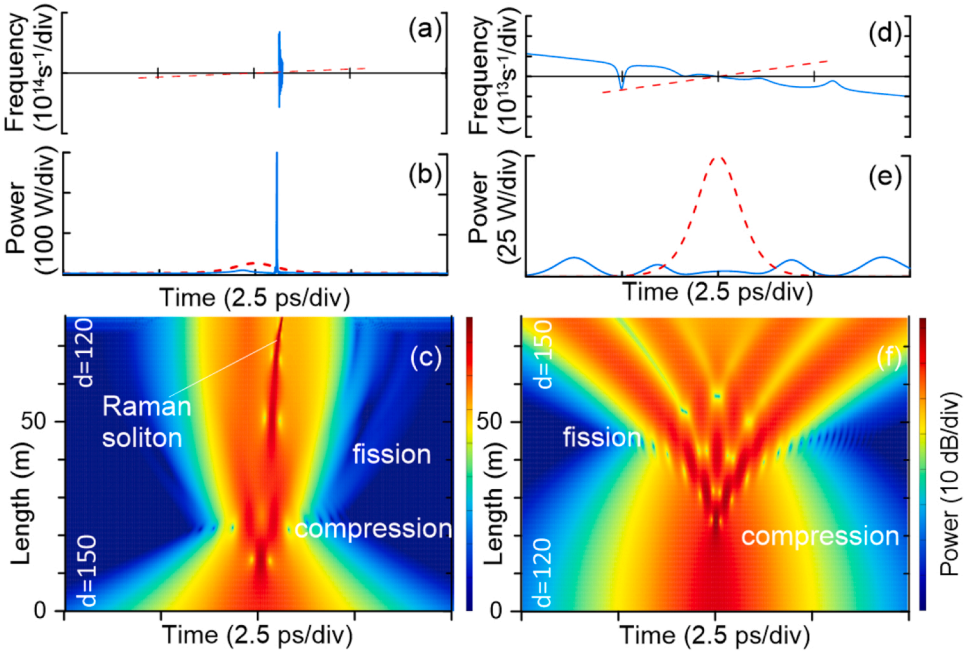

Fig. 7. Propagation of the pump pulse with central wavelength $\lambda = 1530$ nm in dispersion varying fiber. Results of numerical simulations. The pulse propagates in the DDF (a, b, c); or in the DIF (d, e, f). (a, d) Instantaneous frequency at the input (dashed red) and at the output of the fiber (blue solid line). (b,e) Envelopes of the pulse at the input (dashed red) and at the output of the fiber (blue solid line) (c, f) Evolution of the intensity during the pump pulse propagation.

to the experimental data. As we believe, solution of this kind can be proposed as the base for development of new-type fiber-optic photonic logic elements.

The simulations of the second experimental configuration with pump pulse centered at the wavelength of 1063 nm is of significant computational difficulty due to the fact that it is necessary to take into account a large amount of data both in temporal (~ 1 ns) and spectral (more than 10^{15} s^{-1} wide) domains. To reduce computational costs, we limited the consideration to the initial conditions in the form of a frequency-modulated Gaussian pulse $A(t) = \sqrt{P_0}\exp(-(1+iC)t^2/2\tau^2)$ with the duration of $\tau = 100$ps, chirp $C = 1000$ and peak power $P_0 = 1000$W. The simulation window has 2^{18} points with grid step $\Delta t = 2.75$ fs.

The pump pulse evolutions corresponding to propagation in both directions in spectral and temporal domains are shown in Figs. 8 and 9, respectively. A well-observed typical feature of the evolution process in the spectral region is sequential multiple SRS bands, which transfer pump energy to longer wavelengths closer to the region of anomalous dispersion. The part of the radiation that crosses the zero dispersion wavelength (ZDW) decays into a large number of ultrashort Raman solitons with a peak power of several kilowatts. Under the SRS action, these solitons are shifted towards the long-wavelength part of the spectrum.

In the time domain, one can see the optical wave-breaking process beginning near the top of the pulse, where the nonlinear effects are strongest. Several traces of multiple sequential SRS cascades are noticeable near the trailing (right) edge of the pulse as sections with flat frequency modulation. Due to the normal fiber dispersion, the part of radiation with longer wavelengths moves to the leading (left) edge of the pulse. Further, this part of the pulse envelope passes into the region of anomalous dispersion and decays into ultrashort Raman solitons. As one can see, the smoothed shape of the output pulse envelope with a steep leading and flat trailing edge is in good agreement with experimental observations.

Considering the evolution processes for forward and backward pump pulse propagations, we should note that the differences between them are not so prominent. We assume that this is due the fact that generated SC width is much wider than the spectral features of longitudinal dispersion distribution in the fiber sample. Nevertheless, some peculiarities associated with the longitudinal change of the ZDW can be highlighted. When the pump pulse propagates in forward direction, the ZDW shifts towards longer wavelengths providing a gradual broadening of the normal dispersion region. As a result, a smaller part of the pump energy is transferred into the anomalous dispersion region and transformed into the ultrashort solitons. On the contrary, in the case of the fiber with a longitudinally increasing diameter, the ZDW shifts to the left, increasing the region of anomalous dispersion. Thus, a larger part of intense radiation, initially located in the normal dispersion region, can cross the ZDW and enter into the region of anomalous dispersion, forming a wide soliton spectrum. Despite the longitudinal decreasing of the nonlinearity, the simulation results show that the output spectrum obtained for backward pump pulse propagation is significantly wider than otherwise (Fig. 8(a, c)). In addition, change in the ZDW position leads to variation in generation conditions of dispersion waves that appear at the short-wavelength edge of the SC spectrum. Although there are some differences between the simulation results and the experiment explained by the difference in the form of the initial signal, inaccuracies in the specification of fiber parameters and neglecting the frequency dependence of nonlinearity and linear losses, we should note that the simulations are in principal agreement with the experimental data.

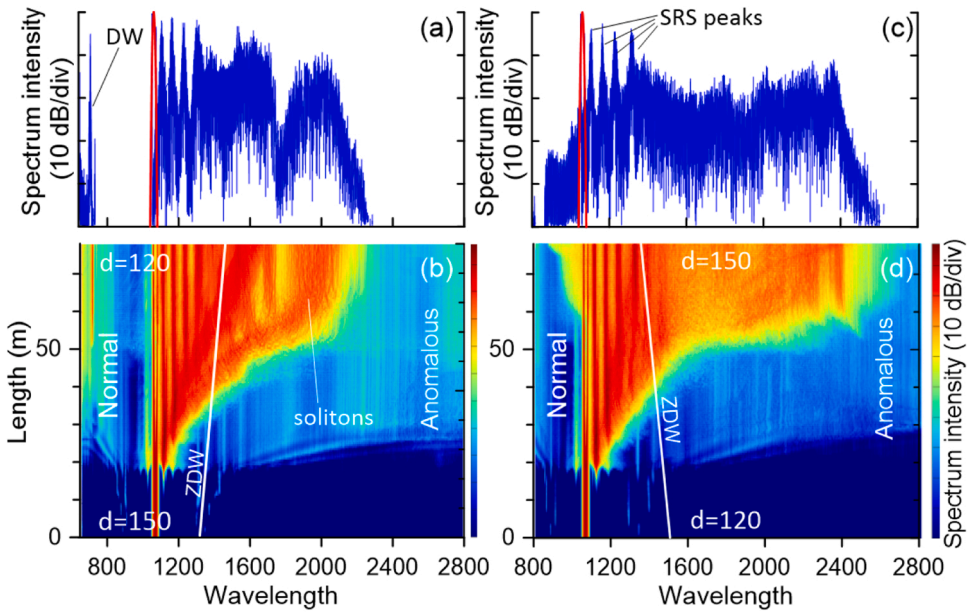

Fig. 8. Propagation of the high-energy pump pulse with central wavelength $\lambda = 1063$ nm in dispersion varying fiber. Results of numerical simulations. Spectra at the input (red) and at the output (blue lines) of fiber with longitudinally decreasing (a) and increasing (c) diameters. The evolution of the spectral intensity during the pump pulse propagation through the fiber with longitudinally decreasing (b) and increasing (d) diameters.

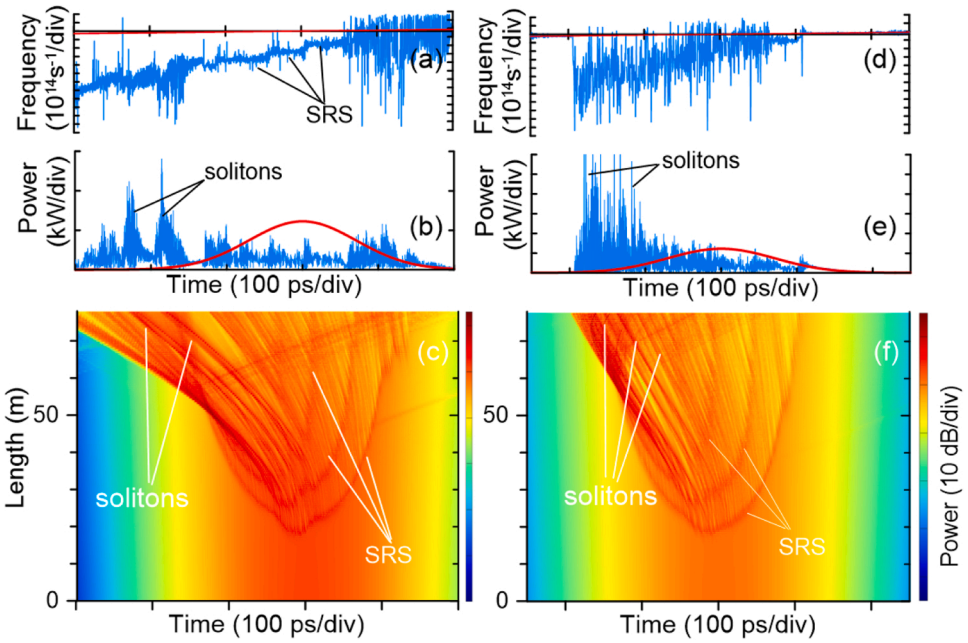

Fig. 9. Propagation of the high-energy pump pulse with central wavelength $\lambda = 1063$ nm in dispersion varying fiber. Results of numerical simulations. Frequency modulation of radiation at the input (red) and at the output (blue lines) of fiber with longitudinally decreasing (a) and increasing (d) diameters. The initial pulse envelope (red) and the radiation intensity at the output (blue lines) of fiber with longitudinally decreasing (b) and increasing (e) diameters. The evolution of the radiation intensity during the propagation of the pump pulse through the fiber with longitudinally decreasing (c) and increasing (f) diameters.

4. Discussion and conclusions

It is known, that the optical fibers with waveguide parameters varying in length according to some predetermined law have substantial applications for optical signal processing and novel fiber laser sources. The key to the stable SC source is a properly designed dispersion profile of the fiber, which allows generating a continuum that could be extremely broad, smooth (less than a few dB of ripple) and stable against input pump noise [13–17, 38, 39]. In this work, we consider two different examples of fiber SC generators based on the same fiber with longitudinally varying diameters.

The considered examples differ by the principal different scale of nonlinear spectrum transformation. The power pump pulse with kW peak power and energy of about hundreds of nJ provides the generation of SC with spectrum width ~ 800 nm in standard uniform fiber [32]. Nevertheless, application of dispersion varying fibers allows to get some special properties of the SC generated. Longitudinal change of the ZDW can be used to control the energy of the soliton part of the pump pulse and to increase the intensity of long- or short-wavelength edges of the SC spectrum.

On the contrary, the evolution of the pump pulse of rather low energy (~ tens of pJ) drastically depends on direction of propagation. The fiber with anomalous dispersion decreasing from the value of about ~ -15 ps^{2}m^{-1} down to the zero can provide the formation of broadband single ultrashort soliton accompanied by low intensity background. This result is radically different from the backward propagation leading to the minimum spectrum broadening of the pump pulse. The observed fundamental difference in direction-dependent propagation properties makes the DDF perspective element of logical photonic circuits.

Development of the management of the SC spectrum by variation of the longitudinal dispersion profile opens the way to solving a number of important problems. It seems appropriate to mention in this context the methods using soliton propagation in a periodically and quasi-periodically dispersion modulated or dispersion oscillating fibers (DOF) [40–42]. In particular, the DOF can be used to change the velocity, amplitude, and number of solitons by changing the pulse parameters as functions of the dispersion modulation period and phase in a fiber [43]. Moreover, it has been explored a novel class of soliton solutions for the nonautonomous NLSE models with linear and harmonic oscillator potentials, which substantially extend the concept of classical solitons and generalize it to the elastically interacting solitons moving with varying amplitudes, speeds, and spectra and adapted to both the external potentials and the dispersion and nonlinearity variations [44].

In fibers with a complex longitudinal profile, the SC generation scenario can be substantially extended. The known scenarios are generation of polychromatic dispersion radiation in a fiber of a special design with longitudinal profile of the zero dispersion wavelength (ZDW) synchronized with “red” Raman shift of a soliton pump pulse [45] or in a fiber with an axially oscillating profile allowing the generating soliton pulse to approach ZDW repeatedly [46]. Therefore, the provided conditions lead to multiplication of the resonant radiation generation points along the fiber length and contribute to almost complete transfer of the pulse energy into a wide dispersion spectrum. In [47] an original way to control simultaneously the wavelength and duration of Raman-shifted solitons

due to longitudinally non-uniform photonic crystal fibers was proposed. In [48] soliton pulse propagation is modeled in a tapered photonic crystal fiber for various taper profiles with the purpose of optimizing the Raman frequency shift. However, the interesting results of this work are limited to the case of a single fundamental soliton propagating in tapered fiber.

To evaluate the wide possibilities of the methods applying the longitudinal fiber profile management, following the basic idea of [48], we shortly consider the spectrum transformation of the pump pulse of the telecom range into the spectrum domain of $2-2.5$ μm employing fibers with special dispersion profile. A more detailed description of the problem can be found in [34]. The original task was to study the spectrum transformation of the pump pulse of telecom range in inhomogeneous fiber and to determinate the optimal longitudinal fiber profile $d(z)$ enabling high efficient energy transfer into the given spectrum range ($\lambda > 2$ μm) required for a number of applications [49,50]. Initially, it seems to be enough to inject a pulse into a fiber with low anomalous dispersion and then match the profile $d(z)$providing the soliton Raman shift without an increase in the local dispersion$D(\lambda)$. To solve the task is convenient to apply the fibers with so-called flattened dispersions. Their dispersion curves for various values of diameters are shown in Fig. 10 (a). Therefore, the task solution is the longitudinal profile of tapered fiber $d(z)$ providing a flat dispersion dependence on the wavelength$D(\lambda)$. Let us consider an example: a transform limited Gaussian pulse with a duration of $\tau_0 = 0.3$ps and peak power of 250 W is injected into the flat dispersion fiber with the initial diameter of $d = 115.5$μm (Fig. 10 (b)).

For the first 20 m of the fiber, the diameter and dispersion of the fiber are not changing. In this fiber section, the initial pulse breaks into a fundamental Raman soliton with a maximum peak power that exhibits a "red" Raman shift and a residual radiation at the pump frequency. The residual pulse peak power is relatively low and its Raman shift is negligible. In this fiber segment, the soliton moving to the right crosses the dispersion curve minimum. After that, the fiber diameter increases synchronously with the Raman soliton wavelength λ_s to maintain the constant current fiber dispersion$D(\lambda)$. To satisfy this condition, one should use a tapered fiber with a longitudinally increasing diameter in such a way that resonant radiation emission point shifts towards longer wavelengths and center of soliton spectrum stays in a certain constant distance (~ 75 nm) from the second "red" zero dispersion ZDW 2 (Fig. 10 (b)). Due to this tapering, the transfer of soliton energy to the dispersive waves in the normal dispersion long-wavelength spectral domain (to the right of ZDW 2) is inefficient. The constant dispersion value at soliton carrier wavelength maintains the constant spectrum width during the pulse propagation. The soliton peak power also tends to be approximately constant.

However, low dispersion value in the first fiber section enhances the generation of resonant dispersive radiation in the normal dispersion short-wavelength domain (to the left of ZDW 1). Even in the first fiber segment, when the compression of the input pulse occurs but the fundamental soliton is not formed yet, one can see the generation of power dispersive wave. As a result, this technique does not allow to move a pulse to the wavelength over 2 μm using a fiber sample with the length of hundreds of meters. Ultimately, at the output of the fiber one can observe rather broad SC spectrum (in the range of 1.3–2 μm) of non-uniform intensity.

For efficient generation of pulses with carrier wavelength over 2 μm, we propose an alternative solution. In our configuration, the initial fiber section has a larger diameter and, consequently, higher anomalous dispersion. As one can see the high dispersion at the fiber beginning decreases the soliton order ($N \propto |D|^{-1/2}$ [35]) thereby allowing: 1) to avoid generation of short-wave resonant radiation at the initial stage; 2) to form a fundamental soliton of higher energy. Next, the fiber diameter has to decrease to avoid an increase of the local dispersion and decrease of the soliton peak power, and then, similar to the described case, the diameter has to increase in order to maintain a constant dispersion at the soliton carrier wavelength.

The spectrum evolution in this configuration is shown in Fig. 10 (c). Similar to the previous case, we take transform-limited Gaussian pulse with the duration of $\tau_0 = 0.3$ ps and peak power of 250 W as the initial pump pulse. In the first fiber section with the length of 11 m and $d(z) = 128.5$ μm ($\beta_2 \approx -17 \mathrm{ps}^2\mathrm{km}^{-1}$) a fundamental soliton separates from the pump pulse. Importantly, in this

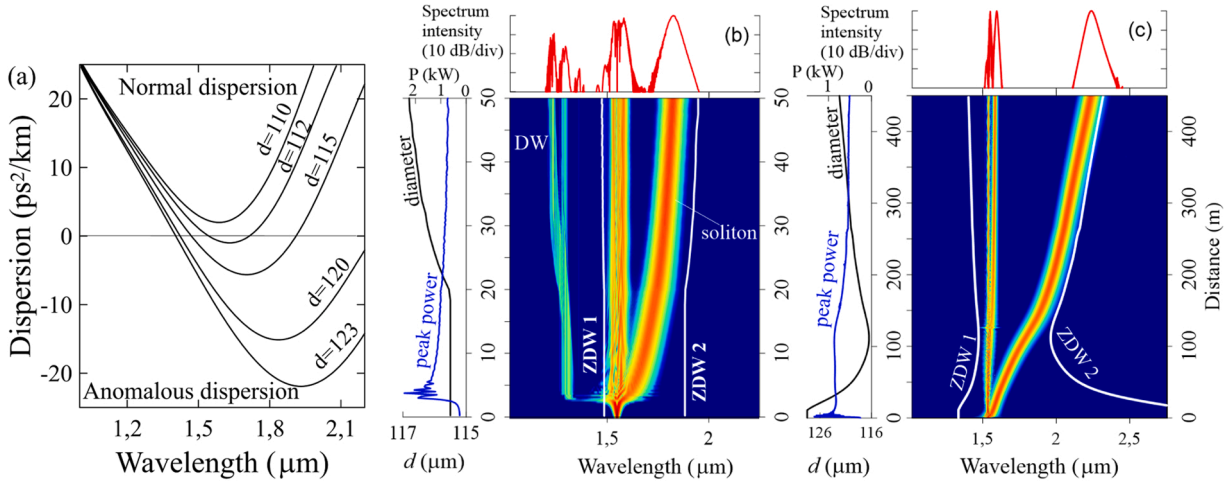

Fig. 10. (a) Dispersion curves for single-mode dispersion flattened fibers of various diameters. (b) Evolution of the pump pulse spectrum in an optical fiber with a diameter increasing with fiber length. Left: changes of the fiber diameter and radiation peak power along the fiber length. Top: radiation spectrum at the fiber output. DW is the dispersion radiation spectrum; ZDW 1 and ZDW 2 are changes of zero-dispersion wavelengths. (c) The same as in (b) but for evolution of the pump pulse spectrum in the optical fiber with a special longitudinal profile.

case, the resonant radiation is not generated. Then, in a 100 m fiber segment, the fiber diameter decreases. In this fiber section, the longitudinal profile of the diameter maintains the soliton peak power constant during the Raman shift. Importantly, the main soliton moving to "red" side goes beyond the frequency minimum of dispersion curve. Passing a short transition zone in the next segment, the fiber diameter smoothly increases ensuring a constant dispersion value at the carrier wavelength. Note, similar to the previous case, in this segment, the soliton peak power is nearly constant. As a result, at the output of 450 m fiber, a spectrum in the range of 2.2–2.3 μm contains more than 60 % of full spectrum energy. Importantly, in contrast to a number of alternative converters [49–51] transforming the pump pulse spectrum into a broadband supercontinuum comprising a dispersive component, in this case, the pump energy is concentrated in a subpicosecond pulse with duration of about 120 fs and peak power of P∼500 W that is of particular interest for many applications.

As a conclusion, we consider a number of specific methods of using fibers with varying longitudinal dispersion profiles for SC generation. The description of direction-dependent pump pulse propagation for the considered configurations, obtained through experimental results and numerical simulations, will be in demand in the development of new SC fiber laser sources and systems of optical signal processing.

Funding

The work is supported by the Ministry of Science and Higher Education of the Russian Federation (project #075-15-2021-581), works on SC generation with the laser sources of telecom range are supported by the Russian Science Foundation #22-12-00396, works on SC generation with the laser sources of 1060nm are supported by the Russian Science Foundation #23-79-30017.

Declaration of Competing Interest

The authors declare that they have no known competing financial interests or personal relationships that could have appeared to influence the work reported in this paper.

Data availability

Data will be made available on request.

References

[1] J.M. Dudley, J.R. Taylor (Eds.), Supercontinuum Generation In Optical Fibers, Cambridge University Press, 2010.
[2] T. Sylvestre, E. Genier, A.N. Ghosh, P. Bowen, G. Genty, J. Troles, J.M. Dudley, Recent advances in supercontinuum generation in specialty optical fibers, JOSA B 38 (12) (2021) F90–F103.
[3] T.S. Saini, T.H. Tuan, T. Suzuki, Y. Ohishi, Coherent mid-IR supercontinuum generation using tapered chalcogenide step-index optical fiber: experiment and modelling, Sci. Rep. 10 (1) (2020) 2236.
[4] S. Lambert-Girard, M. Allard, M. Piché, F. Babin, Differential optical absorption spectroscopy lidar for mid-infrared gaseous measurements, Appl. Opt. 54 (2015) 1647, https://doi.org/10.1364/AO.54.001647.
[5] R. Bartlome, M.W. Sigrist, Laser-based human breath analysis: D/H isotope ratio increase following heavy water intake, Opt. Lett. 34 (2009) 866, https://doi.org/10.1364/ol.34.000866.
[6] A. Reyes-Reyes, Z. Hou, E. van Mastrigt, R.C. Horsten, J.C. de Jongste, M.W. Pijnenburg, H.P. Urbach, N. Bhattacharya, Multicomponent gas analysis using broadband quantum cascade laser spectroscopy, Opt. Express 22 (2014) 18299, https://doi.org/10.1364/OE.22.018299.
[7] S. Dupont, C. Petersen, J. Thøgersen, C. Agger, O. Bang, S.R. Keiding, IR microscopy utilizing intense supercontinuum light source, Opt. Express 20 (2012) 4887, https://doi.org/10.1364/OE.20.004887.
[8] A.B. Seddon, Mid-infrared (IR)—a hot topic: the potential for using mid-IR light for non-invasive early detection of skin cancerin vivo, Phys. Status Solidi B 250 (2013) 1020–1027, https://doi.org/10.1002/pssb.201248524.
[9] D. Stoliarov, A. Koviarov, D. Korobko, D. Galiakhmetova, E. Rafailov, Fibre laser system with wavelength tuning in extended telecom range, Opt. Fiber Technol. 72 (2022), 102994.
[10] T. Ohara, H. Takara, T. Yamamoto, H. Masuda, T. Morioka, M. Abe, H. Takahashi, Over-1000-channel ultradense WDM transmission with supercontinuum multicarrier source, J. Lightwave Technol. 24 (2006) 2311–2317, https://doi.org/10.1109/JLT.2006.874548.
[11] S.V. Smirnov, J.D. Ania-Castanon, T.J. Ellingham, S.M. Kobtsev, S. Kukarin, S.K. Turitsyn, Optical spectral broadening and supercontinuum generation in telecom applications, Opt. Fiber Technol. 12 (2) (2006) 122–147.
[12] D.A. Korobko, O.G. Okhotnikov, D.A. Stoliarov, A.A. Sysolyatin, I.O. Zolotovskii, Broadband infrared continuum generation in dispersion shifted tapered fiber, JOSA B 32 (4) (2015) 692–700.
[13] N. Nishizawa, T. Niinomi, Y. Nomura, L. Jin, Y. Ozeki, Octave spanning coherent supercontinuum comb generation based on Er-doped fiber lasers and their characterization, IEEE J. Sel. Top. Quantum Electron. 24 (3) (2017) 1–9.
[14] M.D. Pelusi, H.F. Liu, Higher order soliton pulse compression in dispersion-decreasing optical fibers, IEEE J. Quantum Electron. 33 (1997) 1430–1439.
[15] T. Okuno, M. Onishi, M. Nishimura, Generation of ultra-broad-band supercontinuum by dispersion-flattened and decreasing fiber, IEEE Photonics Technol. Lett. 10 (1) (1998) 72–74.
[16] F. Lu, W. Knox, Generation of a broadband continuum with high spectral coherence in tapered single-mode optical fibers, Opt. Express 12 (2004) 347–353.
[17] J. Kutz, C. Lynga, B. Eggleton, Enhanced supercontinuum generation through dispersion-management, Opt. Express 13 (2005) 3989–3998.
[18] J.C. Travers, J.M. Stone, A.B. Rulkov, B.A. Cumberland, A.K. George, S.V. Popov, J.R. Taylor, Optical pulse compression in dispersion decreasing photonic crystal fiber, Opt. Express 15 (20) (2007) 13203–13211.
[19] T. Hirooka, M. Nakazava, Parabolic pulse generation by use of a dispersion-decreasing fibre with normal group-velocity dispersion, Opt. Lett. 29 (5) (2004) 498–500.
[20] C. Finot, B. Barviau, G. Millot, A. Guryanov, A. Sysoliatin, S. Wabnitz, Parabolic pulse generation with active or passive dispersion decreasing optical fibers, Opt. Express 15 (24) (2007) 85824–85835.
[21] D. Korobko, O. Okhotnikov, A. Sysolyatin, M. Yavtushenko, I. Zolotovskii, Optical amplifier with tailored dispersion for energy scaling of similaritons, J. Opt. Soc. Am. B 30 (2013) 582–588.

[22] I.O. Zolotovskii, D.A. Korobko, D.I. Sementsov, Formation of parabolic pulses in inhomogeneous fiber optical amplifiers, Phys. Wave Phenom. 21 (2013) 110–117.
[23] V.I. Kruglov, A.C. Peacock, J.D. Harvey, Exact solutions of the generalized nonlinear Schrödinger equation with distributed coefficients, Phys. Rev. E 71 (2005), 056619.
[24] I.S. Panyaev, D.A. Stoliarov, A.A. Sysolyatin, I.O. Zolotovskii, D.A. Korobko, High-frequency pulse train generation in dispersion-decreasing fibre: using experimental data for the metrology of longitudinally nonuniform fibre, Quantum Electron. 51 (5) (2021) 427.
[25] S. Chernikov, D. Richardson, D. Payne, E. Dianov, Soliton pulse compression in dispersion-decreasing fiber, Opt. Lett. 18 (1993) 476–478.
[26] D. Korobko, O. Okhotnikov, I. Zolotovskii, High-repetition-rate pulse generation and compression in dispersion decreasing fibers, J. Opt. Soc. Am. B 30 (2013) 2377–2386.
[27] E.E. Bordon, W.L. Anderson, Dispersion-adapted monomode fiber for propagation of nonlinear pulses, J. Lightwave Technol. 7 (2) (1989) 353.
[28] V.A. Bogatyrjov, M.M. Bubnov, S.L. Semjenov, A.A. Sysoliatin, Length-varying computer-controlled fibre drawing, Meas. Sci. Technol. 5 (1994) 1370.
[29] D.V. Skryabin, A.V. Yulin, Theory of generation of new frequencies by mixing of solitons and dispersive waves in optical fibers, Phys. Rev. E 72 (2005), 016619.
[30] T. Hori, N. Nishizawa, T. Goto, M. Yoshida, Experimental and numerical analysis of widely broadened supercontinuum generation in highly nonlinear dispersion-shifted fiber with a femtosecond pulse, J. Opt. Soc. Am. B 21 (2004) 1969.
[31] A.V. Husakou, J. Herrmann, Supercontinuum generation, four-wave mixing, and fission of higher-order solitons in photonic-crystal fibers, JOSA B 19 (9) (2002) 2171–2182.
[32] I.V. Zhluktova, V.A. Kamynin, D.A. Korobko, A.S. Abramov, A.A. Fotiadi, A.A. Sysoliatin, V.B. Tsvetkov, Broadband supercontinuum generation in dispersion decreasing fibers in the spectral range 900–2400 nm, Photonics 9 (10) (2022) 773.
[33] G. Genty, S. Coen, J.M. Dudley, Fiber supercontinuum sources, JOSA B 24 (8) (2007) 1771–1785.
[34] D.A. Korobko, V. Rastogi, A.A. Sysoliatin, I.O. Zolotovskii, Generation of 2 μm radiation due to single-mode fibers with longitudinally varying diameter, Opt. Fiber Technol. 47 (2019) 38–42.
[35] G.P. Agrawal. Nonlinear Fiber Optics, sixth ed., Academic Press, 2019.
[36] K. Tajima, Compensation of soliton broadening in nonlinear optical fibers with loss, Opt. Lett. 12 (1) (1987) 54–56.
[37] K.R. Tamura, H. Nakazawa, Femtosecond soliton generation over a 32-nm wavelength range using a dispersion-flattened dispersion-decreasing fiber, IEEE Photonics Technol. Lett. 11 (3) (1999) 319–321.
[38] Kunihiko Mori, Hidehiko Takara, Satoki Kawanishi, Analysis and design of supercontinuum pulse generation in a single-mode optical fiber, J. Opt. Soc. Am. B 18 (12) (2001) 1780.
[39] C.X. Yu, H.A. Haus, E.P. Ippen, W. Wong, A.A. Sysoliatin, Gigahertz-repetition-rate mode-locked fiber laser for continuum generation, Opt. Lett. 25 (19) (2000) 1418–1420.
[40] A.A. Sysoliatin, A.K. Senatorov, A.I. Konyukhov, L.A. Melnikov, V.A. Stasyuk, Soliton fission management by dispersion oscillating fiber, Opt. Express 15 (25) (2007) 16302–16307.
[41] C. Finot, J. Fatome, A. Sysoliatin, A. Kosolapov, S. Wabnitz, Competing four-wave mixing processes in dispersion oscillating telecom fiber, Opt. Lett. 38 (24) (2013) 5361–5364.
[42] A.A. Sysoliatin, K.S. Gochelashvili, A.I. Konyukhov, L.A. Melnikov, V.A. Stasyuk, All-optical fiber soliton processing using dispersion oscillating fiber, Laser Phys. Lett. 17 (6) (2020), 065105.
[43] A.I. Konyukhov, E.V. Shchurkin, L.A. Melnikov, A.A. Sysolyatin, K.S. Gochelashvili, On the all-fiber optical methods of the generation and recognition of soliton states, JETP 128 (3) (2019) 384–395.
[44] V.N. Serkin, Akira Hasegawa, T.L. Belyaeva, Nonautonomous solitons in external potentials, PRL 98 (2007), 074102.
[45] C. Milián, A. Ferrando, D.V. Skryabin, Polychromatic Cherenkov radiation and supercontinuum in tapered optical fibers, JOSA B 29 (2012) 589–593.
[46] A. Bendahmane, F. Braud, M. Conforti, B. Barviau, A. Mussot, A. Kudlinski, Dynamics of cascaded resonant radiations in a dispersion-varying optical fiber, Optica 1 (4) (2014) 243–249.
[47] F. Braud, A. Bendahmane, A. Mussot, A. Kudlinski, Simultaneous control of the wavelength and duration of Raman-shifting solitons using topographic photonic crystal fibers, J. Opt. Soc. Am. B 32 (2015) 2146–2152.
[48] A.C. Judge, O. Bang, B.J. Eggleton, B.T. Kuhlmey, E.C. Mägi, R. Pant, C.M. de Sterke, Optimization of the soliton self-frequency shift in a tapered photonic crystal fiber, JOSA B 26 (11) (2009) 2064–2071.
[49] V.A. Kamynin, A.S. Kurkov, V.B. Tsvetkov, Supercontinuum generation in the range 1.6 — 2.4 μm using standard optical fibres, Quantum Electron. 41 (11) (2011) 986–988.
[50] R. Buczynski, H.T. Bookey, D. Pysz, R. Stepien, I. Kujawa, J.E. McCarthy, M.R. Taghizadeh, Supercontinuum generation up to 2.5 μm in photonic crystal fiber made of lead-bismuth-galate glass, Laser Phys. Lett. 7 (9) (2010) 666.
[51] V.A. Kamynin, A.S. Kurkov, V.M. Mashinsky, Supercontinuum generation up to 2.7 μm in the germanate-glass-core and silica-glass cladding fiber, Laser Phys. Lett. 9 (3) (2012) 219.